Evidence for "Magnetic Rotation" in Nuclei: Lifetimes of States in the M1 bands of ^{198,199}Pb

R. M. Clark,[1] S. J. Asztalos,[1] G. Baldsiefen,[2] J. A. Becker,[3] L. Bernstein,[3] M. A. Deleplanque,[1] R. M. Diamond,[1] P. Fallon,[1] I. M. Hibbert,[4] H. Hübel,[2] R. Krücken,[1] I. Y. Lee,[1] A. O. Macchiavelli,[1] R. W. MacLeod,[1] G. Schmid,[1] F. S. Stephens,[1] K. Vetter,[1] R. Wadsworth,[4] and S. Frauendorf[5]

[1]*Lawrence Berkeley Laboratory, Berkeley, California 94720*
[2]*Institut für Strahlen- und Kernphysik, Universität Bonn, Nussallee 14-16 D-53115 Bonn, Germany*
[3]*Lawrence Livermore National Laboratory, Livermore, California 94550*
[4]*Department of Physics, University of York, Heslington, York, YO1 5DD, United Kingdom*
[5]*Institut für Kern- und Hadronenphysik, Forschungszentrum Rossendorf, PF 510119, D-01314 Dresden, Germany*

(Received 20 August 1996)

Lifetimes of states in four of the $M1$ bands in ^{198,199}Pb have been determined through a Doppler-shift attenuation method measurement performed using the GAMMASPHERE array. The deduced $B(M1)$ values, which are a sensitive probe of the underlying mechanism for generating these sequences, show remarkable agreement with tilted axis cranking (TAC) calculations. The results represent clear evidence for a new concept in nuclear excitations: "magnetic rotation." [S0031-9007(97)02583-0]

PACS numbers: 21.10.Tg, 23.20.Js, 23.20.Lv, 27.80.+w

The observation of long cascades of magnetic dipole ($M1$) transitions in the neutron deficient Pb nuclei [1,2] has prompted great interest among nuclear-structure physicists. The properties of the bands are extremely unusual: (i) most of the structures follow the rotational $I(I+1)$ rule over many states despite very low deformations, (ii) the levels are linked by strong $M1$ transitions with weak $E2$ crossover transitions [typical $B(M1)/B(E2)$ ratios $\geq 20-40$ $(\mu_N/e\,\mathrm{b})^2$], and (iii) the ratio $\Im^{(2)}/B(E2)$ is roughly an order of magnitude larger than that for normal or superdeformed bands, indicating that a substantial portion of the inertia is generated from effects other than quadrupole collectivity.

The initial interpretations of the bands [1,2] suggested that they were based on high-K proton configurations (involving $h_{9/2}$ and $i_{13/2}$ orbitals) which induce a small oblate deformation ($\beta_2 \simeq -0.1$), coupled to neutron holes in the $i_{13/2}$ subshell which carry angular momentum aligned with the collective rotational axis. This picture accounts reasonably for the occurrence of the structures, but how can long, regular cascades, which appear rotational, occur when the nucleus develops only a small deformation?

An intuitively appealing description of the behavior of the $M1$ bands arises naturally from the tilted axis cranking (TAC) model [3], and is schematically illustrated in Fig. 1. Near the band head the proton angular momentum vector, $\mathbf{j}_\pi$, is nearly parallel to the symmetry axis while the neutron angular momentum vector, $\mathbf{j}_\nu$, is perpendicular to it. The total angular momentum vector, $\mathbf{J}$, then lies along a tilted axis at an angle θ with respect to the symmetry axis. To generate angular momentum $\mathbf{j}_\pi$ and $\mathbf{j}_\nu$ gradually align along the direction of $\mathbf{J}$ with θ remaining approximately constant. Only a small component of the total angular momentum is from collective rotation (denoted by $\mathbf{R}$ in Fig. 1). If the spin vectors are long and rigid enough then regular $I(I+1)$ sequences are predicted. Since the behavior of $\mathbf{j}_\pi$ and $\mathbf{j}_\nu$ is reminiscent of the closing of a pair of shears this process has been dubbed the "shears mechanism" [2].

The regular sequences of strongly enhanced $M1$ transitions (sometimes called "shears bands") and the TAC picture suggest a new concept—"magnetic rotation" [4]. This arises as a consequence of breaking the intrinsic rotational symmetry by a long magnetic dipole vector (which rotates about $\mathbf{J}$ in the TAC picture described above). This

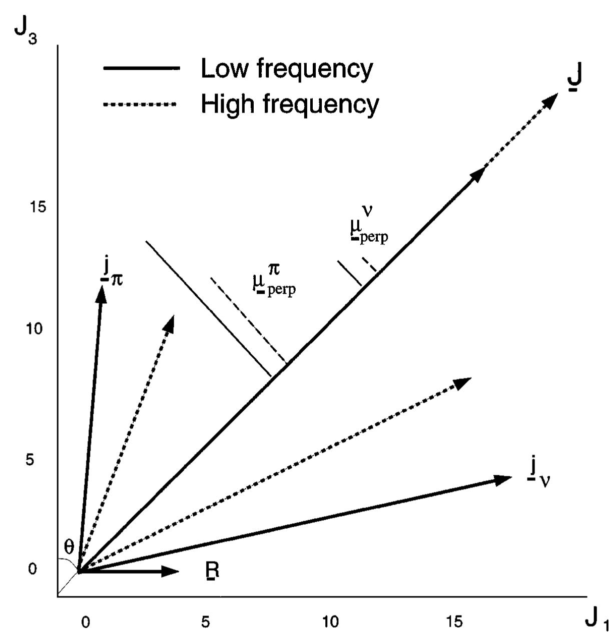

FIG. 1. Schematic representation of the shears mechanism. The labeling is described in the text (vector quantities are denoted by underbars). The solid (dashed) arrows show the approximate coupling at low (high) frequency.

is in direct analogy to the familiar concept of ("electric") rotation when the symmetry is broken by an electric quadrupole resulting from the deformed nuclear charge distribution.

Experimental routhians, angular momenta, and moments of inertia for the bands are well reproduced in the TAC model [2–4]. However, there is a crucially important prediction of the model that remained unconfirmed. Since the $B(M1)$ is determined by the components of the magnetic moments perpendicular to **J** (labeled $\mu_{\text{perp}}^{\nu/\pi}$ in Fig. 1), a characteristic drop in the magnitude of $B(M1)$ is expected with increasing rotational frequency. Previous attempts at deducing $B(M1)$ values through lifetime measurements [5–9] proved inconclusive. Indeed, glaring discrepancies exist between the results for the four $M1$ bands in ^{198}Pb and ^{199}Pb for which measurements had previously been made [5,7,9]. (These bands are bands 1 and 2 in ^{199}Pb, and bands 1 and 3 in ^{198}Pb using the labeling conventions of [1] and [2], respectively. Hereafter, we denote these bands by $^{199}\text{Pb}(1,2)$ and $^{198}\text{Pb}(1,3)$). The deduced $B(M1)$'s for $^{199}\text{Pb}(1,2)$ [9] were roughly twice the values predicted by TAC although the errors were large and the results did suggest a dropoff in $B(M1)$ with increasing frequency. In comparison, the previous results for $^{198}\text{Pb}(1,3)$ [5,7] were a factor of 2 smaller than TAC predictions and one band [^{198}Pb(3)] even showed a sharp rise in $B(M1)$ at the highest rotational frequency. Note, this previous generation of experiments all suffered from relatively poor statistics.

We have performed an experiment to determine lifetimes of states in the $M1$ bands of ^{198,199}Pb. High-spin states in these nuclei were populated simultaneously using the $^{186}\text{W}(^{18}\text{O}, xn)$ reactions at 99 and 104 MeV. The beam, which was accelerated by the 88-Inch Cyclotron of the Lawrence Berkeley Laboratory, was incident on a 12.2 mg/cm^2 thick ^{186}W target for the higher beam energy, while the run at the lower beam energy used a 500 μg/cm^2 ^{186}W foil on a 700 μg/cm^2 Al backing. Gamma rays were detected with the GAMMASPHERE array [10] which for this experiment consisted of 60 large-volume [$\sim$(75–80)% efficient] Ge detectors situated at the following angles relative to the beam: 5 at 31.7°, 5 at 37.4°, 10 at 50.1°, 3 at 58.3°, 1 at 79.2°, 1 at 80.7°, 4 at 90.0°, 1 at 99.3°, 1 at 100.8°, 5 at 121.7°, 10 at 129.9°, 5 at 142.6°, 5 at 148.3°, and 4 at 162.7°. Totals of 4.7×10^8 (quadruples and higher fold) and 1.9×10^9 (triples and higher fold) events were collected using the thick ^{186}W and Al-backed targets, respectively.

The data were sorted into gated, angle-dependent spectra and E_γ-E_γ correlation matrices. All lines in the $M1$ bands of ^{198,199}Pb were at their fully stopped positions in the thick-target data. These data were used to extract branching ratios for the in-band transitions. For the data taken with the Al-backed target, Doppler-broadened line shapes were observed for in-band transitions with $E_\gamma \geq$ 350 keV. Level lifetimes were extracted from these line shapes using the analysis package of Wells and Johnson [11]. The complete stopping was modeled using the prescription discussed in detail by Gascon *et al.* [12]. The tabulations of Northcliffe and Schilling [13] with shell corrections were used for the electronic stopping powers. The detailed slowing-down history of the recoils in the target and backing material was simulated using a Monte Carlo technique (5000 histories with a time step of 0.002 ps) and then sorted according to detector geometry. Calculated line shapes for each transition were

TABLE I. Measured lifetimes, τ (ps), $M1$ branching ratios, B_γ, and reduced transition strengths, $B(M1)$ (μ_N^2) and $B(E2)$ ($e^2\,\text{b}^2$), of states in the bands. I_{SF} is the percentage of side feeding into each state. The errors on the $B(M1)$ and $B(E2)$ values were estimated from the standard (linear) transformation of the errors on the values of τ and B_γ. Note, systematic errors introduced through the treatment of the stopping powers are not included.

	E_γ^{M1} (keV)	E_γ^{E2} (keV)	I_{SF} (%)	τ (ps)	B_γ	$B(M1)$ (μ_N^2)	$B(E2)$ ($e^2\,\text{b}^2$)
^{198}Pb	506	970	41 (11)	$0.20^{+0.05}_{-0.05}$	0.90(2)	$1.85^{+0.46}_{-0.46}$	$0.048^{+0.015}_{-0.015}$
	464	885	36 (8)	$0.14^{+0.03}_{-0.04}$	0.90(2)	$3.14^{+0.84}_{-0.63}$	$0.101^{+0.034}_{-0.029}$
	421	795	30 (8)	$0.15^{+0.03}_{-0.04}$	0.94(2)	$3.36^{+0.71}_{-0.54}$	$0.081^{+0.032}_{-0.030}$
	374	699	21 (6)	$0.14^{+0.03}_{-0.04}$	0.89(3)	$5.90^{+1.70}_{-1.28}$	$0.384^{+0.152}_{-0.133}$
^{198}Pb(3)	471	915	43 (14)	$0.20^{+0.06}_{-0.05}$	0.88(2)	$2.33^{+0.62}_{-0.74}$	$0.081^{+0.025}_{-0.028}$
	444	866	33 (10)	$0.20^{+0.08}_{-0.06}$	0.86(2)	$2.31^{+0.63}_{-0.84}$	$0.107^{+0.033}_{-0.042}$
	422	811	30 (8)	$0.17^{+0.06}_{-0.04}$	0.86(2)	$3.06^{+0.64}_{-0.97}$	$0.173^{+0.044}_{-0.060}$
	389	731	32 (8)	$0.24^{+0.05}_{-0.05}$	0.94(2)	$3.17^{+0.64}_{-0.64}$	$0.094^{+0.037}_{-0.037}$
	342	621	24 (5)	$0.16^{+0.08}_{-0.06}$	0.90(3)	$5.82^{+1.95}_{-2.59}$	$0.487^{+0.218}_{-0.261}$
^{199}Pb(1)	508	967	63 (23)	$0.21^{+0.06}_{-0.05}$	0.86(2)	$1.66^{+0.40}_{-0.48}$	$0.065^{+0.018}_{-0.021}$
	459	870	39 (11)	$0.15^{+0.05}_{-0.04}$	0.93(2)	$2.95^{+0.70}_{-0.87}$	$0.068^{+0.025}_{-0.028}$
	411	774	35 (9)	$0.16^{+0.05}_{-0.04}$	0.90(2)	$4.35^{+1.16}_{-1.45}$	$0.197^{+0.066}_{-0.077}$
	363	679	37 (9)	$0.20^{+0.05}_{-0.05}$	0.90(2)	$4.82^{+1.27}_{-1.27}$	$0.300^{+0.099}_{-0.099}$
^{199}Pb(2)	573	1105	40 (17)	$0.14^{+0.03}_{-0.02}$	0.82(2)	$1.51^{+0.19}_{-0.29}$	$0.050^{+0.009}_{-0.011}$
	532	1014	40 (13)	$0.13^{+0.04}_{-0.03}$	0.85(2)	$1.89^{+0.36}_{-0.47}$	$0.072^{+0.017}_{-0.020}$
	482	912	32 (7)	$0.16^{+0.05}_{-0.03}$	0.90(2)	$2.22^{+0.35}_{-0.59}$	$0.069^{+0.018}_{-0.023}$
	430	807	20 (5)	$0.21^{+0.04}_{-0.03}$	0.89(2)	$2.59^{+0.36}_{-0.47}$	$0.120^{+0.027}_{-0.031}$

obtained assuming (i) feeding into the top of the band through a cascade of five transitions with the same moment of inertia as the in band. The topmost line shape was fitted and the extracted depopulation time of this state was used as an input parameter to extract lifetimes of states lower in the cascade. (ii) Side feeding into each state assuming initially a rotational cascade of five transitions. The intensity of the side feeding was constrained to reproduce that observed experimentally (see Table I). The quadrupole moment and the moment of inertia of the side-feeding band can be regarded as an effective time parameter. The moment of inertia of the side-feeding cascade was varied and it was found that the same lifetimes (within errors) of the in-band states were extracted consistently. The side-feeding lifetimes were always found to be faster (1–2 times) than the in-band lifetimes. The sensitivity of the fit due to side feeding was found to become less lower in the cascade. Simultaneous fits to forward, backward, and transverse spectra were made. Final results were obtained from a global fit of an entire cascade with independently variable lifetimes for each state and associated side feeding. As an example, Fig. 2 shows the experimental data, along with the calculated fits, for the full range of line shapes observed in ^{199}Pb(2).

While this is a standard approach to fitting line shapes, it is not clear *a priori* if the assumptions about the feeding are valid. It proved possible to gate cleanly on the two topmost Doppler-broadened transitions for ^{199}Pb(2), and obtain spectra of sufficient quality to analyze. Gating from above in this way greatly reduces the influence of side feeding on states lower in the cascade. Remaining feeding into the gating states higher in the cascade were treated in the same manner as before. The lifetimes of states, extracted from our analysis of these spectra, were within the errors of those extracted using the method discussed above [see Fig. 3(d)]. This lends greater confidence to our analysis.

We obtained lifetimes for the energy levels in the four bands for which previous measurements had been made (see discussion above). The results are summarized in Table I. The quoted errors reflect the behavior of the χ^2 fit in the vicinity of the best value as the fit parameters are varied, including the effect of side feeding. The errors do not include the systematic errors introduced through the treatment of stopping powers. These may be as large as $\pm 20\%$. However, since ^{198}Pb and ^{199}Pb were formed simultaneously in our reaction the comparative lifetimes of states between the bands are not subject to this effect.

Table I also gives the measured $M1$ branching ratio, $B_\gamma = I_{M1}/(I_{M1} + I_{E2})$, and the estimated $B(M1)$ and $B(E2)$ transition rates deduced from standard formulas [14]. The $\Delta I = 1$ transitions were assumed to be pure $M1$'s. The conversion of the crossover $E2$ transitions is negligible.

Figure 3 shows the resultant $B(M1)$'s plotted as a function of transition energy for each of the bands. For comparison, absolute $B(M1)$ values calculated by means of the TAC model using the parameters given in [9] are also shown for the suggested configurations of each band. The deformation is kept constant close to the equilibrium value for $\omega = 0.3$ MeV. Neutron pairing is included in the calculation since there are several energetically favorable quasineutron excitations possible. However, the proton pairing was neglected since the proton configurations all involve excitations across the large $Z = 82$ shell gap. For the calculation of $B(M1)$ values, a quenching factor of 0.5 was used for the spin g factors. As discussed in [9] the calculated $B(M1)$'s are relatively insensitive to the choice of quenching factor.

Clearly, the $B(M1)$ values deduced from experiment are in excellent agreement with the TAC model predictions.

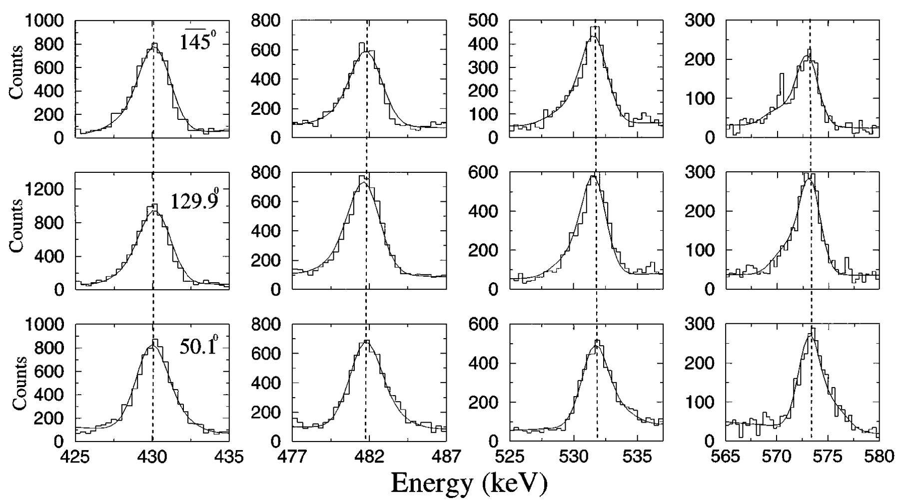

FIG. 2. Experimental data and associated line shape fits for the 573, 532, 482, and 430 keV transitions of ^{199}Pb(2). The spectra were formed from a combination of all double gates on the stopped transitions (377 keV and lower) in the cascade. The rows are labeled by the angles at which the detectors were situated: $\overline{145}°$ refers to a summation of spectra for detectors situated at 142.6° and 148.3°.

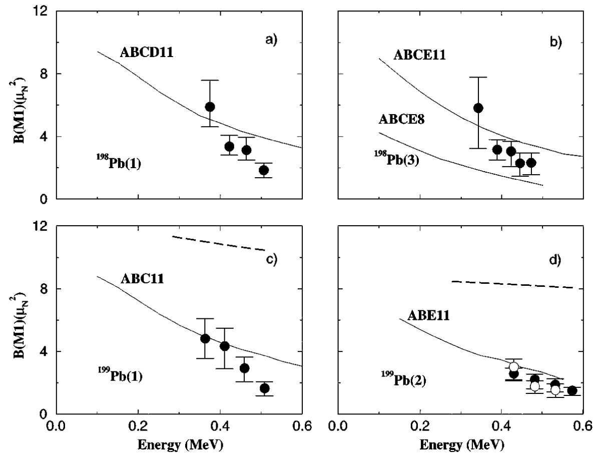

FIG. 3. Experimentally deduced $B(M1)$ (μ_N^2) values, plotted as functions of transition energy (MeV), for the bands in ^{198,199}Pb as discussed in the text. The solid lines are the results of TAC model calculations [9] for the suggested configurations of the bands. A, B, C, D denote the $i_{13/2}$ quasineutrons, E, F the natural parity quasineutrons, and the proton configuration is denoted by its aligned spin (see [2,9]). The dashed lines [parts (c) and (d)] are $B(M1)$ estimates calculated using the treatment of Dönau and Frauendorf [15]. The open circles in part (d) are data points extracted after gating from above.

It should be emphasized here that while an alternative approach of describing the bands in terms of collective oblate structures involving high-K proton configurations coupled to aligned quasineutrons can adequately describe many features such as alignments and angular momenta [1,8] it is impossible to reproduce the experimentally observed behavior of the $B(M1)$'s using this model. To illustrate this, shown in Figs. 3(c) and 3(d) are estimates of the $B(M1)$'s calculated using the Dönau and Frauendorf formula [15], using parameters as discussed in [7]. The empirical numbers are at strong variance with the results of this standard semiclassical treatment, which assumes that the K value is fixed and the alignment is perpendicular to the symmetry axis (no shears mechanism). Both the magnitude and slope of the results are well reproduced by TAC theory. This illustrates that the shears mechanism is a necessary ingredient which must be included if one hopes to describe the observed reduced transition probabilities.

From the experimentally deduced $B(E2)$'s and using the TAC formula [3,9]

$$B(E2) = \frac{15(eQ_0 \sin^2\theta)^2}{128\pi}, \qquad (1)$$

we obtain values of $Q_0 \simeq 3\ e\,$b, which corresponds to an average deformation parameter of $|\beta_2| \simeq 0.1$ [16], consistent with the assumption that the nuclear shape is weakly oblate.

From the observed behavior of the reduced transition probabilities we conclude that our results show that, despite low quadrupole collectivity, regular "rotational" sequences with strongly enhanced magnetic dipole transitions can be explained within the framework of the TAC model. The shears mechanism provides both a qualitatively appealing and quantitatively accurate description of the behavior of the bands in the neutron-deficient Pb nuclei. Moreover, we suggest that our results represent evidence for the concept of magnetic rotation as implied by the shears mechanism. This novel idea extends our conception of the possible modes for nuclear excitations.

We express our gratitude to Dr. John Wells and the crew and staff of the 88-Inch Cyclotron. This work has been supported in part by the U.S. DoE under Contracts No. DE-AC03-76SF00098 (LBL) and No. W-7405-ENG-48 (LLNL). The work of the Bonn group was supported by NATO Grant No. CRG 930496. Funding from the U.K. came from the EPSRC.

[1] R. M. Clark *et al.,* Nucl. Phys. **A562**, 121 (1993), and references therein.
[2] G. Baldsiefen *et al.,* Nucl. Phys. **A574**, 521 (1994), and references therein.
[3] S. Frauendorf, Nucl. Phys. **A557**, 259c (1993).
[4] S. Frauendorf, in Report No. LBL-35687, Vol. 2, p. 52.
[5] T. F. Wang *et al.,* Phys. Rev. Lett. **69**, 21 (1992).
[6] J. R. Hughes *et al.,* Phys. Rev. C **48**, R2135 (1993).
[7] R. M. Clark *et al.,* Phys. Rev. C **50**, 84 (1994).
[8] E. F. Moore *et al.,* Phys. Rev. C **51**, 115 (1995).
[9] M. Neffgen *et al.,* Nucl. Phys. A **595**, 499 (1995).
[10] I. Y. Lee, Nucl. Phys. A **520**, 641c (1990).
[11] J. C. Wells and N. Johnson (private communication). Modified from the original code by J. C. Bacelar.
[12] J. Gascon *et al.,* Nucl. Phys. **A513**, 344 (1990).
[13] L. C. Northcliffe and R. F. Schilling, Nucl. Data Tables **7**, 233 (1970).
[14] H. Ejiri and M. J. A. de Voigt, *Gamma Ray and Electron Spectroscopy in Nuclear Physics* (Oxford University Press, Oxford, England, 1987), p. 504.
[15] F. Dönau and S. Frauendorf, in *Proceedings of the International Conference on High Angular Momentum Properties of Nuclei, Oak Ridge, 1982,* Nucl. Sci. Res. Conf. Series Vol. 4 (Harwood, New York, 1983,) p. 143.
[16] K. E. G. Löbner, M. Vetter, and V. Hönig, Nucl. Data Tables **A7**, 465 (1970).